Inorganic Chemistry
Article

Inorg. Chem. **2010**, *49*, 10833–10839 **10833**
DOI: 10.1021/ic1012523

Topologies of Metal−Organic Frameworks Based on Pyrimidine-5-carboxylate and Unexpected Gas-Sorption Selectivity for CO_2

Jinwoo Seo, Narae Jin, and Hyungphil Chun*

Department of Applied Chemistry, College of Science and Technology, Hanyang University, 1271 Sa-3 dong, Ansan 426-791, Republic of Korea

Received June 23, 2010

A simple and multitopic ligand, pyrimidine-5-carboxylate (pmc), has been used to obtain a series of metal−organic frameworks (MOFs) based on Co^{2+}, Cd^{2+}, and Cu^{2+}. The networks possess well-defined topologies of body-centered-cubic, rutile, and interpenetrated NbO structures, respectively. Among those, $[Cu(pmc)_2]$ possesses a permanent porosity resulting from straight one-dimensional channels of 5.5 Å free passages. Unexpectedly, this porous MOF displays a highly selective sorption behavior for CO_2, and the sorptions of N_2, Ar, O_2, H_2, and CH_4 at two different temperatures are found to be negligible. The results of diffraction and spectroscopic analyses exclude framework dynamics or incomplete evacuation as the origin of the gas-sorption selectivity.

Introduction

Metal−organic frameworks (MOFs) have established the status as a new class of porous materials with potential applications in separation, storage, catalysis, and others.[1] Despite the pessimistic predictions of early days,[2] the facile synthesis, high surface area and porosity, and tunable structures and properties of the novel crystalline materials have attracted researchers to this area. Especially, the tunable nature of MOFs is a great advantage over existing porous materials such as zeolites and has actively been exploited in the form of reticular synthesis[3] or postsynthetic modifications.[4]

Recently, a series of MOFs based on imidazole-related ligands have been reported to possess a chemical stability previously unattainable in most carboxylate-based MOFs.[5] These works highlight the possibility of obtaining new MOFs suited to industrial applications[6] and give us a notion that a particular metal−ligand pair outperforms others with regard to a certain property of MOFs, such as the resistance to hydrolysis. Therefore, future developments in this area require comprehensive knowledge on diverse metal−ligand interactions in network solids. In this context, we have systematically studied MOFs having two types of ligands (dicarboxylate and diamine),[7] and now we have launched a new effort toward porous MOFs that have both amine and carboxylate moieties within the same ligand.[8] Especially, we have become interested in pyrimidine-5-carboxylate (pmc) for its versatile binding modes as a di- or tritopic linker. The ligand is barely known in the field of MOF research.[9]

We report here that pmc is a useful building block that yields new MOFs with well-defined topologies. It is also shown that one of the MOFs not only possesses a permanent porosity but also shows a highly selective sorption behavior for CO_2 over common gases, such as N_2, O_2, Ar, H_2,

*To whom correspondence should be addressed. E-mail: hchun@hanyang.ac.kr.

(1) Recent reviews on the functional aspects of MOFs: (a) Horike, S.; Shimomura, S.; Kitagawa, S. *Nat. Chem.* **2009**, *1*, 695–704. (b) Li, J.-R.; Kuppler, R. J.; Zhou, H.-C. *Chem. Soc. Rev.* **2009**, *38*, 1477–1504. (c) Lee, J.; Farha, O. K.; Roberts, J.; Scheidt, K. A.; Nguyen, S. T.; Hupp, J. T. *Chem. Soc. Rev.* **2009**, *38*, 1450–1459. (d) Murray, L. J.; Dincă, M.; Long, J. R. *Chem. Soc. Rev.* **2009**, *38*, 1294–1314. (e) Férey, G. *Dalton Trans.* **2009**, 4400–4415. (f) Morris, R. E.; Wheatley, P. S. *Angew. Chem., Int. Ed.* **2008**, *47*, 4966–4981. (g) Suh, M. P.; Cheon, Y. E.; Lee, E. Y. *Coord. Chem. Rev.* **2008**, *252*, 1007–1026. (h) Custelcean, R.; Moyer, B. A. *Eur. J. Inorg. Chem.* **2007**, 1321–1340. (i) Maspoch, D.; Ruiz-Molina, D.; Veciana, J. *Chem. Soc. Rev.* **2007**, *36*, 770–818.

(2) O'Keeffe, M. *Chem. Soc. Rev.* **2009**, *38*, 1215–1217.

(3) (a) Caskey, S. R.; Wong-Foy, A. G.; Matzger, A. J. *J. Am. Chem. Soc.* **2008**, *130*, 10870–10871. (b) Tranchemontagne, D. J.; Ni, Z.; O'Keeffe, M.; Yaghi, O. M. *Angew. Chem., Int. Ed.* **2008**, *47*, 5136–5147. (c) Dincă, M.; Long, J. R. *J. Am. Chem. Soc.* **2007**, *129*, 11172–11176. (d) Lin, X.; Jia, J.; Zhao, X.; Thomas, K. M.; Blake, A. J.; Walker, G. S.; Champness, N. R.; Hubberstey, P.; Schröder, M. *Angew. Chem., Int. Ed.* **2006**, *45*, 7358–7364. (e) Sudik, A. C.; Millward, A. R.; Ockwig, N. W.; Côté, A. P.; Kim, J.; Yaghi, O. M. *J. Am. Chem. Soc.* **2005**, *127*, 7110–7118. (f) Kaye, S. S.; Long, J. R. *J. Am. Chem. Soc.* **2005**, *127*, 6506–6507. (g) Ma, B.-Q.; Mulfort, K. L.; Hupp, J. T. *Inorg. Chem.* **2005**, *44*, 4912–4914. (h) Chun, H.; Dybtsev, D. N.; Kim, H.; Kim, K. *Chem.—Eur. J.* **2005**, *11*, 3521–3529.

(4) Wang, Z.; Cohen, S. M. *Chem. Soc. Rev.* **2009**, *38*, 1315–1329 and references cited therein.

(5) Park, K. S.; Ni, Z.; Côté, A. P.; Choi, J. Y.; Huang, R.; Uribe-Romo, F. J.; Chae, H. K.; O'Keeffe, M.; Yaghi, O. M. *Proc. Natl. Acad. Sci. U.S.A.* **2006**, *103*, 10186–10191.

(6) Czaja, A. U.; Trukhan, N.; Müller, U. *Chem. Soc. Rev.* **2009**, *38*, 1284–1293.

(7) (a) Chun, H.; Jung, H.; Seo, J. *Inorg. Chem.* **2009**, *48*, 2043–2047. (b) Chun, H. *J. Am. Chem. Soc.* **2008**, *130*, 800–801. (c) Chun, H.; Moon, J. *Inorg. Chem.* **2007**, *46*, 4371–4373.

(8) (a) Chun, H.; Seo, J. *Inorg. Chem.* **2009**, *48*, 9980–9982. (b) Chun, H.; Jin, N. *Bull. Korean Chem. Soc.* **2009**, *30*, 1405–1406.

(9) Sengupta, O.; Chakrabarty, R.; Mukherjee, P. S. *Dalton Trans.* **2007**, 4514–4516.

Published on Web 11/09/2010

Scheme 1. Three MOFs Based on pmc and Their Network Topologies

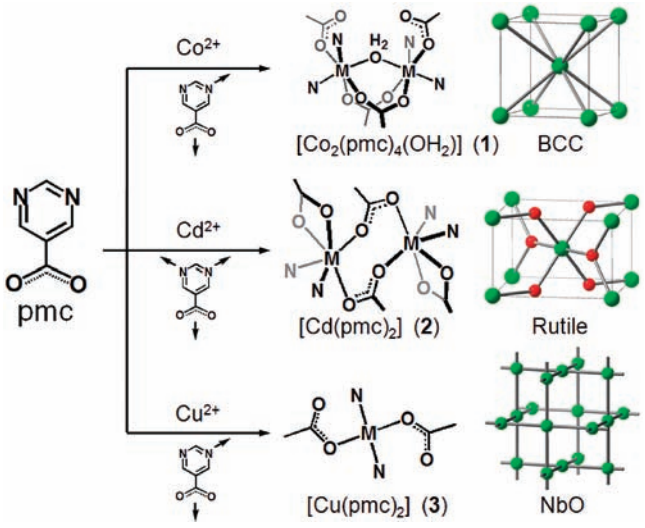

and CH_4. The basic building units and topologies of the three-dimensional (3D) nets derived from pmc ligands are shown in Scheme 1. The body-centered-cubic-type structure of the densely packed MOF $[Co_2(pmc)_4(OH_2)]\cdot$DMF (**1**; DMF = *N*,*N*-dimethylformamide) has been reported elsewhere.[8b]

Experimental Section

Materials and Methods. All of the reagents and solvents were obtained from commercial sources. Thermogravimetric analysis (TGA) data were obtained on a SCINCO S-1000 instrument with a heating rate of 5 °C min^{-1} in air (Figures S1 and S2 in the Supporting Information). IR data were recorded on KBr pellets with a Varian FTS 1000 instrument (Figure S3 in the Supporting Information). In order to measure the IR spectrum for **3**·CO_2, the KBr pellet of evacuated **3** was heated to 100 °C under vacuum and then exposed to CO_2 gas (~2 atm) at room temperature. After 1 h, the pellet was subjected to measurements in ambient air. The powder X-ray diffraction (PXRD) patterns were recorded on a Bruker D8 Advance system equipped with a Cu-sealed tube (λ = 1.541 78 Å) and a computer-controlled heating stage inside a sealed chamber that can be evacuated. The variable-temperature measurements were performed by heating and holding the sample at a target temperature for at least 30 min.

$[Cd(pmc)_2]$ (2). $Cd(NO_3)_2\cdot 4H_2O$ (0.027 g, 0.087 mmol) and Hpmc (0.020 g, 0.16 mmol) were dissolved in DMF (2.6 mL). After stirring for 2 h, the solution was sealed in a glass vial and then heated to 112 °C for 43 h. The product crystallized as colorless thin plates when the solution was allowed to stand at room temperature for 1 day (0.022 g, 75.8%). Calcd for $[Cd(C_5H_3N_2O_2)_2]\cdot 2H_2O$: C, 30.44; H, 2.55; N, 14.20. Found: C, 30.57; H, 2.44; N, 13.65%.

$[Cu(pmc)_2]\cdot{}^2/_3$DMF (3·DMF). $Cu(NO_3)_2\cdot{}^5/_2H_2O$ (0.084 g, 0.36 mmol) and Hpmc (0.089 g, 0.72 mmol) were dissolved in DMF (6.0 mL). After stirring for 1 h, the solution was sealed in a glass vial and then heated to 98 °C for 21 h. Hexagonal column-shaped crystals of deep-purple color formed. The as-synthesized crystals were collected, washed with DMF and CS_2, and soaked in CS_2 before drying under vacuum for 18 h at room temperature (0.092 g, 82.5%). Calcd for $[Cu(C_5H_3N_2O_2)_2]\cdot{}^2/_3C_3H_7NO\cdot 0.5H_2O$: C, 39.22; H, 3.20; N, 17.79. Found: C, 38.90; H, 2.81; N, 17.80%.

X-ray Crystallography. Single crystals of **2** and **3**·DMF were directly picked up from the mother liquor, attached to a glass fiber, and transferred to a cold stream of liquid nitrogen (−100 °C) for data collection. The full hemisphere data were collected on a Siemens SMART CCD diffractometer with Mo Kα radiation (λ = 0.710 73 Å). After data integration (*SAINT*)[10] and semiempirical adsorption correction based on equivalent reflections (*SADABS*),[11] the structures were solved by direct methods and subsequent difference Fourier techniques (*SHELXTL*).[12] All of the non-hydrogen atoms were refined anisotropically, and hydrogen atoms were added to their calculated positions. The solvent DMF of **3**·DMF sits on a special position with rotational disorder over three positions. The summary of the crystal data and structure refinements is shown in Table 1. The data for **3**·toluene were measured with synchrotron radiation on a 6B MX-I ADSC Quantum-210 detector with a silicon (111) double-crystal monochromator at the Pohang Accelerator Laboratory, Pohang, Kyungbuk, Korea. The ADSC Quantum-210 ADX program (version 1.92)[13] was used for data collection, and HKL2000 (version 0.98.699)[14] was used for cell refinement, reduction, and absorption correction. The unit cell parameter *a* of **3**·toluene was found to be twice that of **3**·DMF probably because of the solvent ordering inside the channels. See the Supporting Information for details.

Table 1. Summary of Crystal Data and Structure Refinements

	2	**3**·DMF
formula	$Cd(C_5H_3N_2O_2)_2$	$Cu(C_5H_3N_2O_2)_2\cdot{}^2/_3C_3H_7NO$
fw	358.59	358.46
cryst syst	monoclinic	rhombohedral
space group	$P2_1/c$	$R\bar{3}$
unit cell dimens	a = 7.959(2) Å b = 9.180(2) Å c = 15.796(3) Å β = 104.492(2)°	a = 21.466(2) Å c = 7.772(1) Å
V (Å^3)	1117.5(4)	3101.6(6)
Z	4	9
ρ_{calcd} (g cm^{-3})	2.131	1.727
μ (mm^{-1})	1.971	1.616
F(000)	696	1635
cryst size (mm^3)	0.32 × 0.27 × 0.20	0.50 × 0.20 × 0.15
reflns collected	6434	6357
indep reflns (R_{int})	2648 (0.0391)	1677 (0.0168)
T_{max}/T_{min}	0.6939/0.5711	0.7936/0.4988
data/restraints/param	2648/0/188	1677/12/121
GOF on F^2	1.257	1.430
R1, wR2 [$I > 2\sigma(I)$]	0.0390, 0.0971	0.0463, 0.1091
R1, wR2 (all data)	0.0461, 0.0992	0.0481, 0.1097
largest difference peak/hole (e Å^{-3})	0.960/−0.934	0.618/−1.279

Gas-Sorption Studies. Brunauer−Emmett−Teller gas-sorption isotherms were measured with a Belsorp Mini-II (BEL Japan, Inc.) at one of the following temperatures: liquid nitrogen (77 K), liquid argon (87 K), or slush baths of dry ice−isopropyl alcohol (195 K) or ice−water (273 K). The gases used were of extra-pure quality (N50 for Ar, CO_2, and N_2, N60 for H_2, and N45 for O_2). As-synthesized samples of **3** (~100 mg) were guest-exchanged with CS_2 and, prior to the measurements, evacuated under a dynamic vacuum (10^{-3} Torr) at room temperature for 12 h. A typical weight loss by this pretreatment method is 15−19%. The equilibrium criteria were set consistent throughout all of the measurements (changes in adsorption amounts of less than 0.1 cm^3 g^{-1} within 180 s); however, increasing the equilibrium time to 540 s did not affect the results. All of the measurements were repeated at least twice from fresh

(10) *SAINT*, version 6.45; Bruker AXS Inc.: Madison, WI, 2003.
(11) Sheldrick, G. M. *SADABS*, version 2.10; University of Göttingen: Göttingen, Germany, 2003.
(12) Sheldrick, G. M. *Acta Crystallogr., Sect. A: Found. Crystallogr.* **2008**, *64*, 112–122.
(13) Arvai, A. J.; Nielsen, C. *ADSC Quantum-210 ADX Program*; Area Detector System Corp.: Poway, CA, 1983.
(14) Otwinowski, Z.; Minor, W. In *Methods in Enzymology*; Carter, C. W., Jr., Sweet, R. M., Eds.; Academic Press: New York, 1997; Vol. *276*, Part A, p 307.

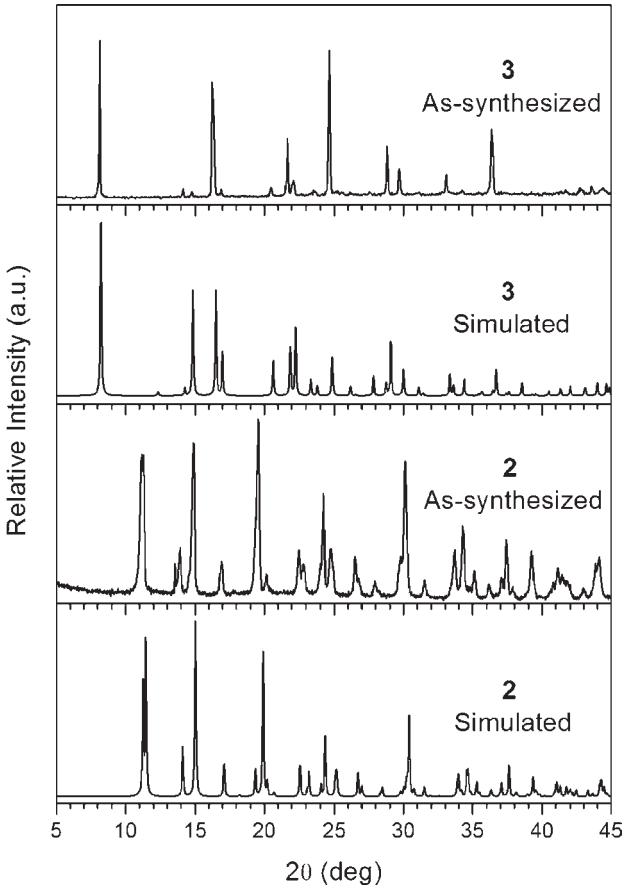

Figure 1. PXRD patterns of as-synthesized **2** and **3** compared to their simulations based on single-crystal data.

samples and are reproducible. Complete sorption isotherms for Ar, CH_4, H_2, N_2, and O_2 are shown in Figures S9−S13 in the Supporting Information.

Results and Discussion

Solvothermal reactions of H(pmc) and nitrates of Co^{2+}, Cd^{2+}, and Cu^{2+} in DMF produce single crystals having compositions of **1**, **2**, and **3**·DMF, which are deduced from the X-ray crystal structure analysis. Elemental analysis and PXRD studies independently confirm the bulk purity of the products. In the PXRD patterns shown in Figure 1, a number of strong diffractions are observed in positions expected from the single-crystal data.

The structure of **1** is based on a secondary building unit (SBU) in which two octahedral Co^{2+} ions are bridged by an aqua ligand and two carboxylate moieties of pmc ligands. Overall, the dinuclear SBU is supported by eight pmc ligands that act as simple ditopic linkers. Therefore, **1** is characterized as a uninodal 8-connected net, and the topology underlying the net is found to be body-centered-cubic (net symbol bcu).[15] The details of the structure and properties have been reported elsewhere.[8b]

The SBU of **2** is a dimetal unit supported by two asymmetric carboxylate bridges (Figure 2a). Each Cd^{2+} ion is further coordinated by three pmc ligands with one chelating carboxylate and two pyrimidyl nitrogen atoms. The dimetal SBU thus can be simplified as a 6-connecting node. While the nitrogen atoms of the bridging pmc ligands do not participate in the binding of Cd^{2+} ions, nonbridging pmc ligands fully utilize their donor atoms to coordinate Cd^{2+} ions, rendering themselves 3-connecting nodes. Therefore, the 3D framework of **2** is a binodal 6,3-connected net with vertex figures of distorted octahedral and trigonal-planar geometries (Figure 2b). The most important net of this kind is rutile (TiO_2, net symbol rtl), and that is indeed the topology underlying the net of **2** (Figure 2c,d). The framework of **2** is densely packed and crystallizes without the presence of any solvent molecules in the crystal lattice.

The structure of **3** is built upon mononuclear Cu^{2+} coordinated by four pmc ligands in a square-planar geometry (Figure 3a). The ligand may be considered as a simple ditopic linker because one of the two nitrogen atoms does not directly bind to a metal ion (see below). This means that **3** is a uninodal 4-connected net based on square-planar nodes, and simplification of the framework reveals that the inorganic prototype NbO (net symbol nbo) is the underlying topology (Figure 3b). As noted by O'Keeffe and co-workers,[16] the nbo topology is one of the five regular nets and is the only possible 3D net from square nodes and simple ditopic linkers.

The overall packing structure of **3** is a 2-fold interpenetrating nbo net (Figure 3c). The two interpenetrating nets are chemically and crystallographically equivalent. A close examination of the crystal structure shows that the square-planar Cu^{2+} ion in one net is weakly bonded to "noncoordinating" nitrogen atoms of pmc ligands in the interpenetrating net (Figure S4 in the Supporting Information). The Cu···N distance is 3.2 Å, and the N···Cu···N vector is tilted about 21.6° against the vertical axis of the square-planar geometry.

This interpenetration mode of **3** deserves additional comments. First, the interpenetration is not simply a result of mechanical interlocking, but there are significant chemical interactions between Cu^{2+} in one net and the "idle" nitrogen atoms of another. Therefore, a dynamic motion, such as slippage of the interpenetrating nets upon guest exchange or evacuation, is unlikely. Second, in principle the interpenetration in **3** may be avoided if we could remove the nonbonded N···Cu···N interactions. Therefore, we attempted to replace pmc with nicotinate (pyridine-3-carboxylate) in the same synthesis; however, the synthetic condition has not been found yet. Finally, the 3D pore system of the original nbo net is reduced to one-dimensional (1D) channels as a result of the interpenetration in **3** (Figure 3d). The hexagonal channels run along the *c* axis of **3**, which is the [111] direction of the ideal nbo lattice with cubic symmetry. The hexagonal 1D channels have a relatively uniform cross-sectional area, and an imaginary sphere of 5.5 Å diameter would pass through the channels without touching the Connolly surface (1.4 Å) of the framework.[17] The helical triangular channels are too small to be occupied. The accessible free voids in **3** are estimated to be about 29% of the total crystal volume.

The thermal behavior of framework material **3** is evaluated by TGA and variable-temperature PXRD (vT-PXRD). The result of TGA for as-synthesized **3** shows a weight loss of less than 5% until about 250 °C, from which decomposition of

(15) O'Keeffe, M.; Peskov, M. A.; Ramsden, S. J.; Yaghi, O. M. *Acc. Chem. Res.* **2008**, *41*, 1782–1789.

(16) Friedrichs, O. D.; O'Keeffe, M.; Yaghi, O. M. *Acta Crystallogr., Sect. A: Found. Crystallogr.* **2003**, *59*, 22–27.

(17) Connolly, M. L. J. *Appl. Crystallogr.* **1983**, *16*, 548–558. The calculation was carried out using: *Materials Studio*, version 4.3; Accelrys, Inc.: San Diego, CA, 2008.

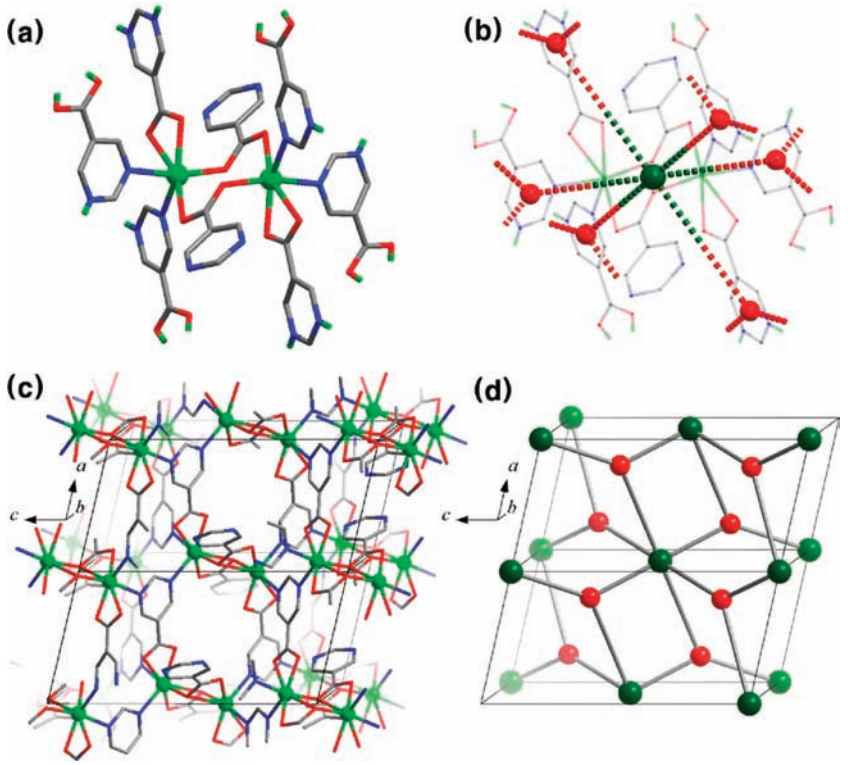

Figure 2. X-ray crystal structure of **2**: (a) dinuclear SBU; (b) simplification of the SBU and ligand as 6- and 3-connecting nodes, respectively; (c) partially expanded framework and (d) its simplified view according to part b.

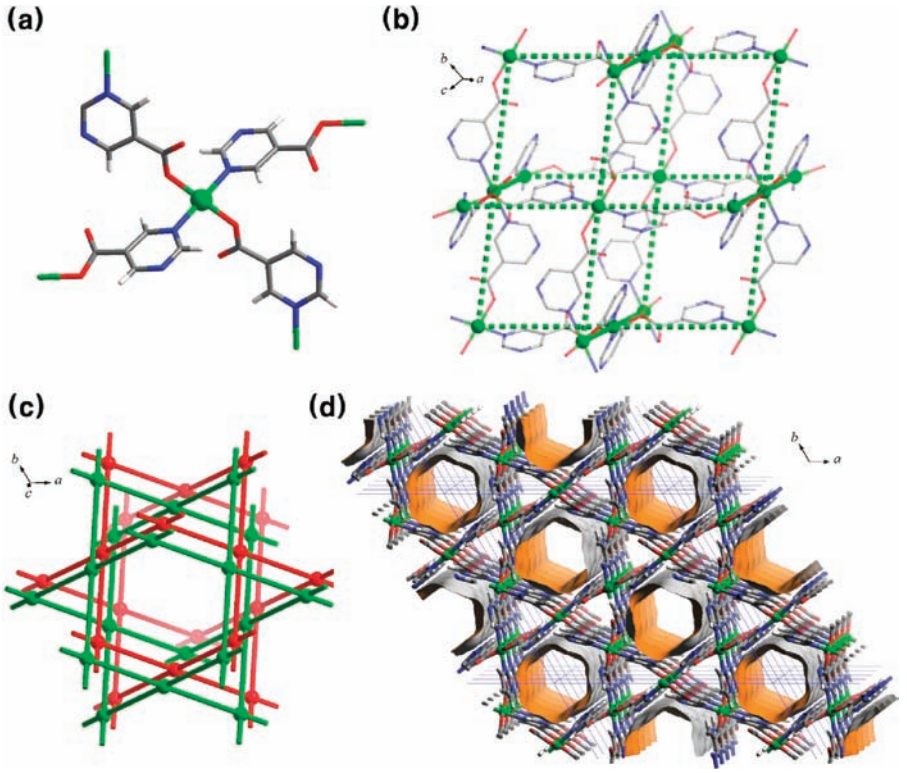

Figure 3. X-ray crystal structure of **3**: (a) coordination environment around the square-planar Cu^{II} center; (b) partially expanded view showing a single net of NbO topology; (c) simplified network revealing the 2-fold interpenetration; (d) overall packing structure showing hexagonal 1D channels.

the framework commences (Figure S2 in the Supporting Information). After complete evacuation following guest exchange (see below), the bulk product displays PXRD patterns that corroborate well with the simulation based on the single-crystal data. Also, the measurements of vT-PXRD show characteristic reflections even at 200 °C without a

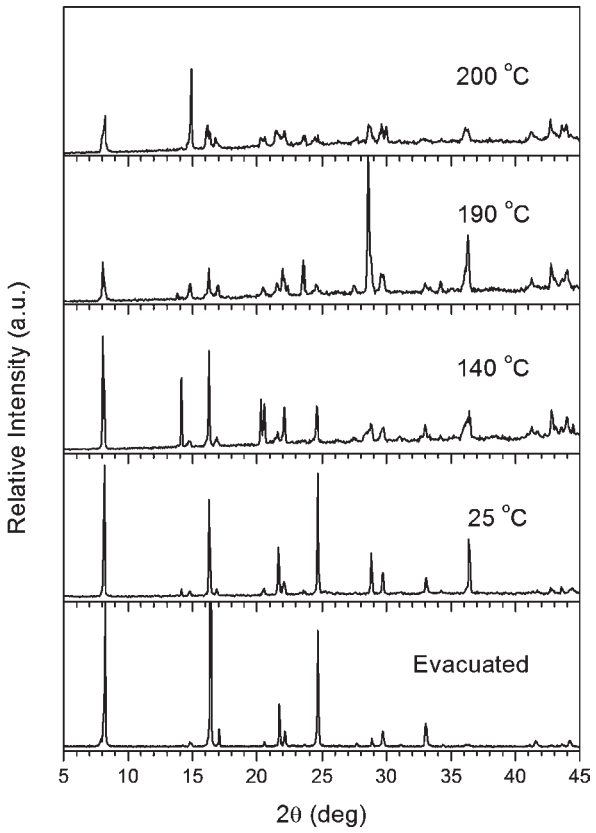

Figure 4. PXRD patterns of **3** measured after complete evacuation and upon heating from room temperature under vacuum.

pronounced shift of the Bragg angles (Figure 4). This compelling evidence establishes the stability and rigidity of the evacuated framework of **3**.

We also determined the crystal structure of **3** after heating of the as-synthesized crystals to 150 °C under vacuum for 12 h. The atomic coordinates and thermal parameters of the framework atoms changed little (Figure S5 in the Supporting Information), and the electron counts for the solvent regions decreased only about 20% (from 257 to 205 electrons per unit cell).[18] These results imply that the guest DMF molecules in as-synthesized **3** are practically occluded within the hexagonal channels (Figure S7 in the Supporting Information) and may not be removed simply by thermal evacuation.

The hygroscopic stability of the porous material **3** was examined by soaking the crystals in deionized water. The dark-purple crystals of **3** gradually crack down to light-blue specimens within hours. Some crystals of the hydrolyzed product were large enough to determine the X-ray structure, and they were found to be a simple complex $[Cu(pmc)_2(OH_2)_4]$,[19] where pmc is an N-bonded monodentate ligand (Figure 5). The hydrolysis product, however, regenerates **3** when it was heated to 100 °C in DMF. Both the hydrolyzed complex and regenerated **3** are phase-pure according to PXRD analysis. Therefore, **3** may be viewed as a "recyclable" porous material.[20] We note that the hydrolysis experiment simulates rather an extreme condition aimed to test the stability of **3** against atmospheric moisture.

The straight 1D channels of **3** having the free passage of 5.5 Å should be accessible to small guest molecules, and therefore we measured the sorptions of N_2, O_2, Ar, H_2, CO_2, and CH_4 for samples pretreated by different methods. To our surprise, however, no gas was found to adsorb in a significant amount when the as-synthesized or guest-exchanged materials (CH_3CN or CH_3OH) were evacuated at 100−150 °C. Suspecting an incomplete exchange of the synthesis solvent, we then used CS_2 as the solvent to exchange the occluded DMF molecules in **3**.[21] As evidenced by IR spectroscopy (Figure 6), the characteristic ν(C=O) band of DMF (1686 cm^{-1}) in as-synthesized **3** completely disappears, and the strong asymmetric stretching band of CS_2 appears at 1518 cm^{-1} for CS_2-exchanged samples. Again, the latter peak disappears when the CS_2-exchanged sample of **3** is put under vacuum at room temperature, implying that a complete and thorough evacuation of **3** can be achieved.

A bulk sample activated by this method shows PXRD patterns that perfectly match the simulation and those of fresh samples (Figure 4). Therefore, evacuation of **3** does not cause movement of the interpenetrating nets or collapse of the open framework.

The inability of CH_3CN or CH_3OH to exchange the included DMF molecules, which is contrasted to CS_2, is not the result of size exclusion. We present, as evidence, the X-ray crystal structure of **3**·toluene that was obtained after soaking of single crystals of **3**·DMF in toluene (Figure S8 in the Supporting Information). In the structure, the toluene molecules are ordered, forming extensive $\pi-\pi$ and CH$-\pi$ interactions inside the channels surrounded by aromatic pyrimidyl rings. Therefore, enhanced noncovalent interactions seem to be the major driving force for the guest-exchange processes.

Having established the optimal activation condition, we measured the sorption isotherms again for various gases after evacuation of the CS_2-exchanged samples of **3**. As shown in Figure 7, a significant amount of CO_2 is adsorbed at 195 and 273 K.

Adsorption of CO_2 at 195 K shows a type I behavior typical for microporous materials but is marked by a pronounced hysteresis between the adsorption and desorption, which suggests the presence of kinetically hindered pores. The total pore volume estimated from the saturated sorption of CO_2 is 0.13 $cm^3\ g^{-1}$, meaning a porosity of 19% based on the crystallographic density. This value is significantly lower than the expected value of 28−29%.

In the mean time, adsorptions of N_2, O_2, Ar, H_2, and CH_4 at two different temperatures are very low. In fact, adsorptions for these gases are almost negligible (< 5 $cm^3\ g^{-1}$) except for Ar at 195 K and CH_4 at 273 K. A potential instrumental failure or measurement error is safely ruled out because the results have been successfully reproduced in more than two independent measurements using freshly prepared samples.

In general, a selective adsorption occurs when the pore size approaches the critical dimensions[22] or kinetic diameters[23] of

(18) Spek, A. L. *PLATON, a multipurpose crystallographic tool*; Utrecht University: Utrecht, The Netherlands, 2001.

(19) Aakeröy, C. B.; Desper, J.; Levin, B.; Valdés-Martínez, J. *Inorg. Chim. Acta* **2006**, *359*, 1255–1262.

(20) (a) Lan, A.; Li, K.; Wu, H.; Kong, L.; Nijem, N.; Olson, D. H.; Emge, T. J.; Chabal, Y. J.; Langreth, D. C.; Hong, M.; Li, J. *Inorg. Chem.* **2009**, *48*, 7165–7173. (b) Gándara, F.; Gomez-Lor, B.; Gutiérrez-Puebla, E.; Iglesias, M.; Monge, M. A.; Proserpio, D. M.; Snejko, N. *Chem. Mater.* **2008**, *20*, 72–76.

(21) It was inspired by the supercritical processing of MOFs: Nelson, A. P.; Farha, O. K.; Mulfort, K. L.; Hupp, J. T. *J. Am. Chem. Soc.* **2009**, *131*, 458–460.

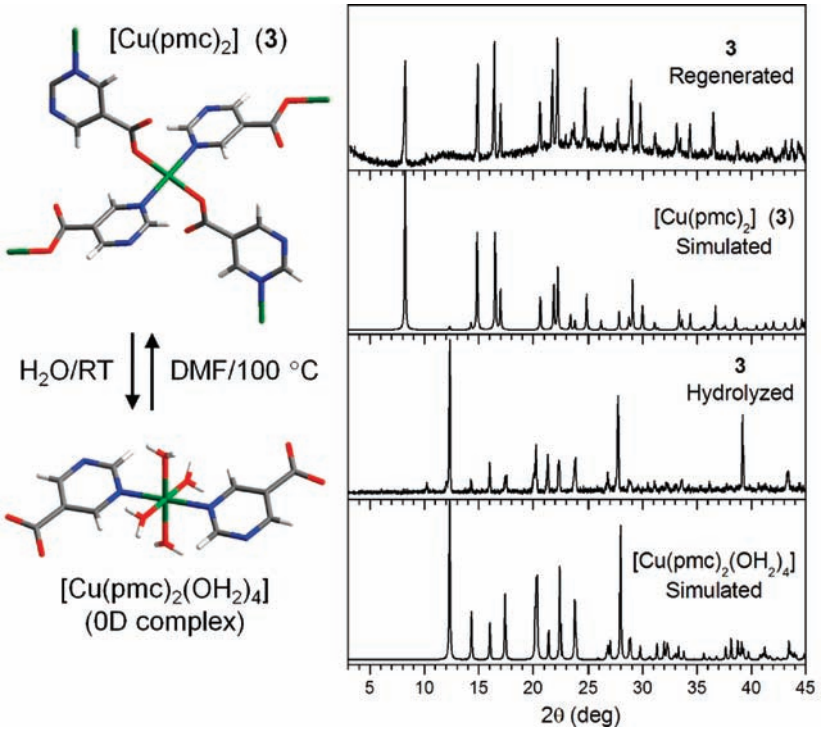

Figure 5. Hydrolysis of **3** into a simple complex and its regeneration to the 3D MOF monitored by PXRD measurements.

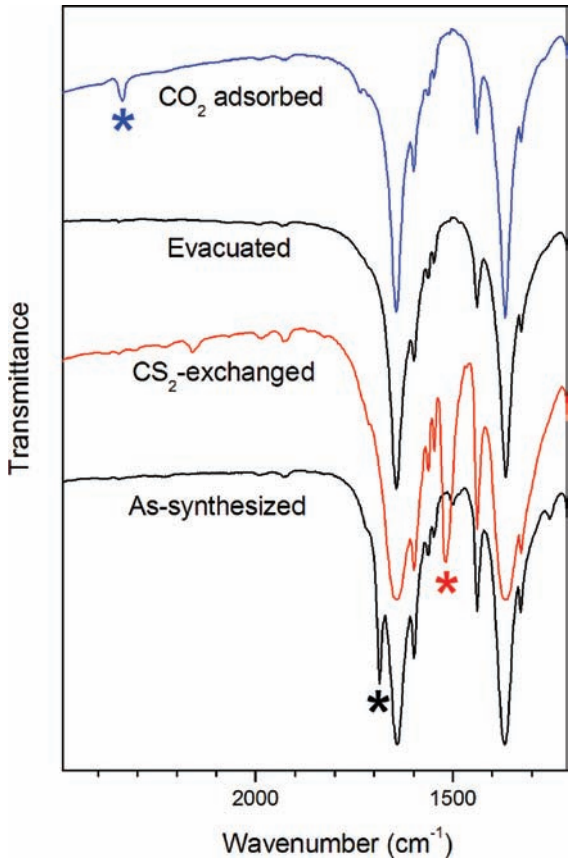

Figure 6. Fourier transform IR spectra for various samples of **3**. Asterisks denote $\nu(C{=}O)_{DMF}$, $\nu(CS_2)$, and $\nu(CO_2)$ bands from bottom to top, respectively.

adsorptive gases. For MOFs with pores that are seemingly large enough for the free passage of small gases, this situation may be encountered when the framework is dynamic with respect to guest-exchange or removal processes. The distortion of organic/inorganic building blocks, movements of interpenetrating nets, or conformational changes of organic ligands are common causes for the dynamic properties of MOFs.[24] An incomplete evacuation of included solvents in the framework may also have the same effect of reducing pore sizes.[25]

Interestingly, the porous MOF **3** fits none of the above profiles.[26] That is, the open channels (5.5 Å) are sufficiently large compared to gas molecules used in this study, which are smaller than 4 Å, the framework is rigid and robust with respect to evacuation, the interpenetrating nets are unlikely to show dynamic motion, and the guest molecules are thoroughly exchanged and completely removed. The results of TGA, vT-PXRD, and single-crystal X-ray and IR spectroscopy collectively support this analysis.

The only plausible explanation for the observed gas-sorption data should be based on the kinetic aspects of the sorption measurements. The diameter of the uniform 1D channels in **3** (5.5 Å) is much smaller than the bilayer thickness of most gas molecules (e.g., 7.3 Å for N_2), and therefore diffusion of adsorptive molecules and adsorption equilibrium will be very

(22) Webster, C. E.; Drago, R. S.; Zerner, M. C. *J. Am. Chem. Soc.* **1998**, *120*, 5509–5516.
(23) Breck, D. W. *Zeolite Molecular Sieves*; Wiley: New York, 1974; p 636.
(24) Such MOFs are extensively cited in refs 1a and 8a.
(25) (a) Ma, S.; Sun, D.; Wang, X. S.; Zhou, H. C. *Angew. Chem., Int. Ed.* **2007**, *46*, 2458–2462. (b) Ma, S.; Wang, X. S.; Collier, C. D.; Manis, E. S.; Zhou, H. C. *Inorg. Chem.* **2007**, *46*, 8499–8501. (c) Navarro, J. A. R.; Barea, E.; Salas, J. M.; Masciocchi, N.; Galli, S.; Sironi, A.; Ania, C. O.; Parra, J. B. *Inorg. Chem.* **2006**, *45*, 2397–2399.
(26) Similar cases have been reported, albeit without exhaustive evidence to rule out the dynamic nature of frameworks. See: (a) Yoon, J. W.; Jhung, S. H.; Hwang, Y. K.; Humphrey, S. M.; Wood, P. T.; Chang, J. S. *Adv. Mater.* **2007**, *19*, 1830–1834. (b) Zou, Y.; Hong, S.; Park, M.; Chun, H.; Lah, M. S. *Chem. Commun.* **2007**, 5182–5184.

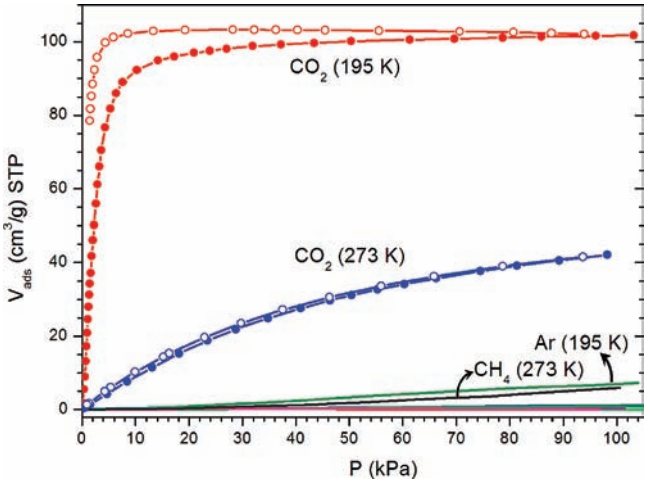

Figure 7. Gas-sorption isotherms for **3**. Unlabeled data are those for N_2 and H_2 at 77 K, O_2 and Ar at 87 K, and N_2, H_2, O_2, and CH_4 at 195 K. See the Supporting Information for details. Filled and open symbols in CO_2 isotherms are adsorption and desorption, respectively.

slow inside the 1D channels because of overlapping potentials from opposite walls. When the diffusion is too slow within a reasonable time frame (see the Experimental Section), the gas sorption at cryogenic temperatures may not be observed. This is especially true for 1D channels with uniform dimensions because a few strongly adsorbed molecules at the pore entrance may block further adsorption. At 195 K, the diffusion and equilibrium is accelerated. At the same time, however, N_2, O_2, Ar, and H_2 molecules carry too much thermal energy to physically adsorb on the pore surface at 195 K. In the case of CO_2, adsorption is favored because of strong adsorptive−adsorptive and adsorptive−adsorbent interactions originating from the permanent and high quadrupole moment of CO_2.[27] The relatively small kinetic diameter of the molecule (3.3 Å) may also have contributed to the accelerated diffusion, but even diffusion of CO_2 inside the pores appears to experience some restrictions, judging from the presence of hysteresis in the sorption isotherms.

In view of practical applications, the highly selective sorption behavior of porous phase **3** may be used to develop packing materials or membranes[28] for capturing or filtering off CO_2 from the atmosphere.[29] The fully evacuated sample of **3**, in the form of a KBr pellet, can uptake and hold CO_2 at room temperature as shown by the $\nu(CO_2)$ band (2338 cm^{-1}) in the IR spectrum that was measured after exposure of the KBr pellet of **3** to a CO_2 atmosphere (Figure 6).

In conclusion, we showed that pmc acts as a simple ditopic or planar tritopic linker to produce 3D MOFs with well-defined topologies. $Cu(pmc)_2$ has a charge-neutral open framework based on interpenetrating nbo nets, and the void framework is stable and rigid. The 3D net is hydrolyzed to give a simple complex in water, but the process can be reversed simply by heating in DMF. The recyclable porous material with straight channels discriminates N_2, O_2, Ar, H_2, and CH_4 but not CO_2 in the gas-sorption experiments. We believe that the slow kinetics for diffusion and adsorption equilibrium within the narrow 1D channels is responsible for the observed selectivity.

Acknowledgment. This research was supported by the Basic Science Research Program through the National Research Foundation of Korea funded by the Ministry of Education, Science and Technology (Grant 2009-0087194). We thank the Pohang Accelerator Laboratory for beamline use (2009-1063-05). H.C. is grateful to Prof. K. Kim (POSTECH, Korea) for allowing access to PXRD.

Supporting Information Available: Details of the crystal structures for **3** and **3**·toluene, TGA plots, complete IR spectra, gas-sorption isotherms for Ar, CH_4, H_2, N_2, and O_2 at 77, 87, 195, and/or 273 K, and crystallographic information files (CIF). This material is available free of charge via the Internet at http://pubs.acs.org.

(27) A similar analysis has been proposed for a porous MOF showing selective sorption of CO_2 over N_2 and O_2: Maji, T. K.; Matsuda, R.; Kitagawa, S. *Nat. Mater.* **2007**, *6*, 142–148.

(28) (a) Li, Y.-S.; Liang, F.-Y.; Bux, H.; Feldhoff, A.; Yang, W.-S.; Caro, J. *Angew. Chem., Int. Ed.* **2010**, *49*, 548–551. (b) Venna, S. R.; Carreon, M. A. *J. Am. Chem. Soc.* **2010**, *132*, 76–78.

(29) Selected examples from recent literature for MOFs showing the selective sorption of CO_2: (a) Nakagawa, K.; Tanaka, D.; Horike, S.; Shimomura, S.; Higuchi, M.; Kitagawa, S. *Chem. Commun.* **2010**, *46*, 4258–4260. (b) Phan, A.; Doonan, C. J.; Uribe-Romo, F. J.; Knobler, C. B.; O'Keeffe, M.; Yaghi, O. M. *Acc. Chem. Res.* **2010**, *43*, 58–67. (c) Demessence, A.; D'Alessandro, D. M.; Foo, M. L.; Long, J. R. *J. Am. Chem. Soc.* **2009**, *131*, 8784–8786. (d) Caskey, S. R.; Wong-Foy, A. G.; Matzger, A. J. *J. Am. Chem. Soc.* **2008**, *130*, 10870–10871. (e) Thallapally, P. K.; Tian, J.; Kishan, M. R.; Fernandez, C. A.; Dalgarno, S. J.; McGrail, P. B.; Warren, J. E.; Atwood, J. L. *J. Am. Chem. Soc.* **2008**, *130*, 16842–16843. (f) Llewellyn, P. L.; Bourrelly, S.; Serre, C.; Filinchuk, Y.; Férey, G. *Angew. Chem., Int. Ed.* **2006**, *45*, 7751–7754.